Journal of Power Sources 195 (2010) 3928–3932

Contents lists available at ScienceDirect

Journal of Power Sources

journal homepage: www.elsevier.com/locate/jpowsour

Short communication

Solar photovoltaic charging of lithium-ion batteries

Thomas L. Gibson, Nelson A. Kelly *

General Motors Research and Development Center, Mail Code 480-106-269, 30500 Mound Road, Warren, MI 48090-9055, USA

ARTICLE INFO

Article history:
Received 23 November 2009
Received in revised form
17 December 2009
Accepted 18 December 2009
Available online 28 December 2009

Keywords:
Solar photovoltaic
Lithium-ion battery
Optimization
Renewable energy

ABSTRACT

Solar photovoltaic (PV) charging of batteries was tested by using high efficiency crystalline and amorphous silicon PV modules to recharge lithium-ion battery modules. This testing was performed as a proof of concept for solar PV charging of batteries for electrically powered vehicles. The iron phosphate type lithium-ion batteries were safely charged to their maximum capacity and the thermal hazards associated with overcharging were avoided by the self-regulating design of the solar charging system. The solar energy to battery charge conversion efficiency reached 14.5%, including a PV system efficiency of nearly 15%, and a battery charging efficiency of approximately 100%. This high system efficiency was achieved by directly charging the battery from the PV system with no intervening electronics, and matching the PV maximum power point voltage to the battery charging voltage at the desired maximum state of charge for the battery. It is envisioned that individual homeowners could charge electric and extended-range electric vehicles from residential, roof-mounted solar arrays, and thus power their daily commuting with clean, renewable solar energy.

1. Introduction

General Motors is pursuing an aggressive strategy for introducing electric powertrains into future vehicles, including extended-range electric vehicles (EREV) and fuel-cell electric vehicles (FCEV). In order to obtain the full environmental and other benefits of EREV and FCEV, the production of electricity and hydrogen needs to shift from fossil-based technology to technologies based on renewable resources, such as solar photovoltaic (PV) electrical energy. Solar energy has the potential to supply an ever increasing portion of the world's energy supply, and is the only energy source that can supply the additional electric power that the world will need over the next several decades in a manner that will protect the environment and be sustainable [1–4]. The first EREV to be introduced by General Motors is the Chevrolet Volt, and it will utilize Li-ion batteries. The storage of solar energy for vehicle propulsion and the advantages of Li-ion batteries as the storage medium is a very active field of research [5–8] that will be greatly expanding in the future.

Renewable electricity could be provided for recharging EREV batteries from wind power, hydroelectric, or nuclear power plants. However, these sources would be centralized in certain areas and not as widely distributed as solar PV power which could be installed for recharging vehicles at most homes. These non-solar sources require conversion to AC power and transmission through the electric power grid which leads to energy losses and lower efficiencies.

In order to compare the benefits of various fuels and energy sources, the complete system efficiency for powering an electric vehicle should be considered, including energy production and storage. For PV solar power using various system designs, the energy efficiency of driving battery or fuel-cell powered electric vehicles includes the following components.

On site solar direct current charging of EREV:

$$\text{system efficiency} = \text{PV efficiency} \times \text{DC charging efficiency} \quad (1)$$

Solar grid-tied charging of EREV:

$$\text{system efficiency} = \text{PV efficiency} \times \text{inverter efficiency} \times \text{transmission efficiency} \times \text{charge controller efficiency} \times \text{DC charging efficiency} \quad (2)$$

Onsite solar to hydrogen FCEV:

$$\text{system efficiency} = \text{PV efficiency} \times \text{electrolyzer efficiency} \times \text{fuel cell efficiency} \quad (3)$$

Using these equations, the efficiency of solar energy conversion to electricity for the power train of an electric vehicle built with

* Corresponding author at: General Motors R&D Center, MC 480-106-269, Chemical Science and Material Systems Laboratory, 30500 Mound Road, Warren, MI 48090-9055, USA. Tel.: +1 586 986 1623; fax: +1 586 986 1910.
E-mail address: nelson.a.kelly@gm.com (N.A. Kelly).

0378-7753/$ – see front matter © 2010 Elsevier B.V. All rights reserved.
doi:10.1016/j.jpowsour.2009.12.082

each of the three basic systems can be estimated using data from the National Research Council [9] and National Renewable Energy Laboratory [10]. Direct current solar charging depends only on the PV solar to electric efficiency, currently about 16% under typical operating conditions and the DC current charging efficiency of the Li-ion batteries, nearly 100%, so that the overall system efficiency approaches 16% (Eq. (1)). The solar grid-tied charging also includes inverter efficiency of 93–97%, and charge controller (rectifier) efficiency of 97%, so that system efficiency is reduced to 13.5% (Eq. (2)) even if "copper losses" from resistance in the added transmission lines are neglected. The solar production of hydrogen to drive a fuel-cell electric vehicle is even less efficient since it includes an electrolyzer, which is typically 60–70% efficient, and a PEM fuel cell, which is about 50% efficient, to make electricity for the vehicle so that the overall system efficiency is less than 6% (Eq. (3)).

However, hydrogen is still a preferable energy carrier as it can be stored in large amounts (several kg) as compressed gas and utilized in fuel cells for both stationary [11] and transportation applications [12], where its end use only results in the formation of water vapor. The amount of energy stored in the battery of an EREV, for example, 16 kWh in a fully charged Chevrolet Volt, is much less than the energy stored in a hydrogen-fueled FCEV with a full tank, such as the Chevrolet Equinox FCEV that holds 4.2 kg of hydrogen (total LHV of approximately 140 kWh). The EREV electric-only driving range of the Chevrolet Volt is expected to be 40 miles (using 8 kWh of battery energy), and the range of the hydrogen powered Chevrolet Equinox FCEV is 160–200 miles. If a hydrogen fuel cell and plug-in hybrid system are combined to drive an electric vehicle then both the short range commute and extended-range road trip can be powered with clean, renewable solar energy thus optimizing the reduction of greenhouse gas emissions.

As an example of a smaller application, a one-vehicle hydrogen fueling system was constructed at the GM Proving Ground in Milford, MI [13]. At that site, a set of four arrays with a solar PV module area of approximately 47 m^2 and a power output of 7.6 kW are used to electrolyze water to produce ~0.5 kg of high-pressure hydrogen gas per day—enough hydrogen to drive an FCEV about 30 km per day. The GM Solar Hydrogen Fueling System consists of a solar PV system small enough to fit on a residential roof, that powers an electrolyzer, storage, and dispensing (ESD) system for fueling an FCEV. The PV-ESD system was designed and built [13] using an optimization technique developed in our laboratory, in which the PV maximum power point was matched to the electrolyzer operating voltage [14]. In the present work, we will utilize a similar technique to study and optimize the solar charging of lithium-ion batteries. A residential solar PV system can thus be used simultaneously to power electric vehicles both by plug-in battery charging (EREV) and hydrogen fueling (FCEV). This experimental system provides a proof of concept for an EREV home scale solar charging station as well as a home hydrogen fueling system for future FCEV owners.

2. Experimental

2.1. Solar powered battery charging

Lithium-ion (Li-ion) battery modules (series strings of cells from A123 Systems, Watertown, MA) [15] with 10-, 12-, 13-, 14-, 15-, and 16-cells in series were constructed by bolting together the individual cell assemblies (Table 1). The modules were immobilized in custom made plastic trays and protected from short circuiting between the cell tabs by polyurethane spacers that prevented any movement of a battery string within its tray. The positive and negative terminals of the battery module were connected directly to the output cables of the PV system using low resistance copper wires and to a data acquisition (DAQ) system or to Fluke multi-meters for voltage and current measurements.

Table 1
Battery cell specifications (A123 Systems high power lithium-ion battery cells) [15].

Specification	Value
Cell type	Lithium iron phosphate ($LiFePO_4$)
Type no.	ANR26650-M1
Model no.	AS400059-001
Operational voltage	3.3 V
Nominal capacity	2.3 Ah
Cell dimensions	26 mm OD × 65.5 mm ht
Cell assembly mass	72 g
Max tab current	100 A continuous
Recommended charge voltage	3.6 V
Recommended float-charge voltage	3.45 V
Recommended cut-off current (100% SOC)	0.05 A
Max. recommended charge voltage	3.8 V
Max. allowable charge voltage	4.2 V
Max. continuous charge current (−20 to 60 °C)	10 A
Recommended discharge cut-off voltage	2.0 V
Max. discharge current	60 A
Max. recommended cell temperature	70 °C
Max. allowable cell temperature	85 °C

2.1.1. Battery module construction and characterization

Each battery module was constructed by connecting the desired number of A123 cells in series by tightening 0.5-in. steel bolts through the positive and negative nickel alloy terminals or tabs on the ends of the cell assemblies which consist of a positive pole (the outer metal can) and a negative pole (the cap). Series strings of 10-, 12-, 13-, 14-, 15-, and 16-cells were made [15]. The cells and modules were characterized in the laboratory by fully charging the cells to their maximum charge voltage 3.8–4.2 V/cell using a conventional battery charger (Powerizer Universal Smart Battery Charger) and then discharging the cells to their minimum voltage (2.0 V/cell) by connecting them to an appropriate load bank such as one or more 16 Ω, 300 W Arcol oil filled resistors (Mouser Electronics). The voltages of individual cells in a series string were balanced by using the charger and load bank to bring all the cells to the same state of charge (SOC) as shown by their voltage (discharged: 2.5 V/cell; fully charged: 4.0 V/cell). The charge capacity of a module in Ah was determined by subtracting the discharged state from the full charge calculated by measuring the current during charging (or discharging) the batteries while timing the procedure.

2.1.2. Solar modules

A single Sanyo HIP-190BA3 PV module was used to charge the battery modules. Under standard test conditions (STC), the Sanyo modules have a short-circuit current of 3.75 A (Table 2). One of the PV modules was connected to the battery module being tested and the DC current was measured using a current shunt and a data acquisition system. The array containing the module was adjusted

Table 2
Electrical, solar to electrical efficiency, and temperature coefficient specifications supplied by the manufacturer for Sanyo HIP-190BA3 modules under standard test conditions, STC (1000 W m^{-2}, 25 °C, AM1.5 solar spectrum) and typical operating conditions (52 °C) [16].

Parameter	Module value (STC)	Module value (52 °C)
Maximum power, P_{max}, watts	190	175
Maximum power point voltage, V_{mpp}, volts	54.8	50.2
Maximum power point current, I_{mpp}, amperes	3.47	3.49
Open circuit voltage, V_{oc}, volts	67.5	62.0
Short-circuit current, I_{sc}, amperes	3.75	3.77
Module efficiency, %	16.1	14.8
Solar cell efficiency, %	18.5	17.0
Temperature coefficient (P_{max}), % °C^{-1}	−0.30	−0.30
Temperature coefficient (V_{oc}), V °C^{-1}	−0.169	−0.169
Temperature coefficient (I_{sc}), mA °C^{-1}	0.86	0.86

to a fixed tilt angle of 57° (latitude + 15°) during the measurements which were all made during the summer of 2008. More details on the solar PV system are contained elsewhere [13].

2.1.3. Data acquisition system

The data acquisition system (DAQ) utilized National Instruments, NI (Austin, TX) hardware and software (LabVIEW, version 8) as described elsewhere [13]. In brief, the PV solar irradiance ($W\,m^{-2}$), temperature, system current, and system voltage were recorded onto the computer hard drive with a date and time stamp every 20 s and read into Excel for analysis.

2.1.4. Battery module tests

The voltage and current of individual Li-ion cells or battery modules were monitored during charging/discharging cycles by using either the solar and DAQ systems at the GM Proving Ground in Milford, MI [13] or with calibrated Fluke model 8808A and 179 RMS multi-meters in our laboratory at the GM R&D Center in Warren, MI. Temperature levels of the Li-ion cells were checked with dedicated temperature sensors. At the beginning of all charging experiments, the battery modules were fully discharged (<1% SOC).

3. Results and discussion

3.1. Battery module measurements

3.1.1. Battery state of charge and module capacity

Battery state of charge (SOC) and module capacity were calculated from the measurements made during charging/discharging cycles by inserting the current and time in Eq. (4) to determine the increase in battery charge and plotting the module voltage versus the added charge (Fig. 1):

$$\text{charge increase} = \text{current} \times \text{time} \tag{4}$$

The battery module capacity in Ah is equal to the charge needed to increase the SOC from a fully discharged state to a fully charged state as shown when plotting the charge versus time (Fig. 2). The maximum charge (100% SOC) at which the battery voltage reaches the recommended charge voltage and the current decreases to the recommended cut-off level represents the battery charge capacity. The maximum allowable voltage was reached at 4.2 V/Li-ion cell, and the battery capacity was found to be 2.35 Ah. The capacity of each battery module determined by performing a series of charging and discharging tests in the laboratory. For strings of cells with 10–16-cells in series (33.5–53.5 V battery modules), the average cell voltage during charge and discharge cycles was 3.37 V, and the pack capacity was consistently 2.35 Ah. The measured charging capacity and discharging capacities of the battery modules were equal within ± 1% (coulombic efficiency = 1). This result confirmed that the charge efficiency and discharge efficiency of Li-ion batteries are nearly 100%, as also reported by others [17,18]. The module energy for strings of from 10 to 16 A123 cells in series varied from 79 to 126 Wh.

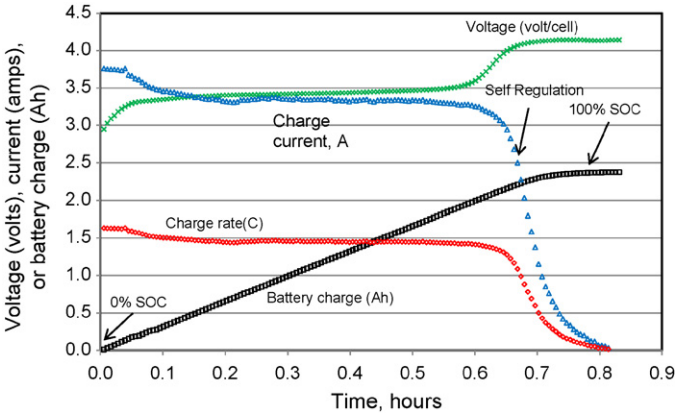

Fig. 2. Solar charging of a 15-cell lithium-ion battery module—voltage per cell, current, charge rate, and battery charge capacity as a function of time.

The rate of battery charging is determined by the fraction of full charge capacity (defined as a unit of 1 C) per hour (in the case of A123 cells, Eq. (5)):

$$C = \left(\frac{\text{charge rate}}{2.35\,\text{Ah}}\right) \times 1\,\text{C} \tag{5}$$

3.1.2. Solar energy to battery charge conversion efficiency

The solar energy to charge conversion efficiency over each time interval in the experimental data set can be calculated from the average voltage, the charge increase (see Eq. (4)), the time step between successive observations in the data set (typically 20 s), and average solar irradiance using Eq. (6):

$$\text{efficiency}\,(\%) = \frac{\text{avg. voltage}\,(\text{V}) \times \text{charge increase}\,(\text{Ah})}{\text{avg. solar irradiance}\,(\text{W m}^{-2}) \times \text{PV area}(\text{m}^2) \times \text{time interval}\,(\text{s}) \times 1/3600\,(\text{s h}^{-1})} \times 100 \tag{6}$$

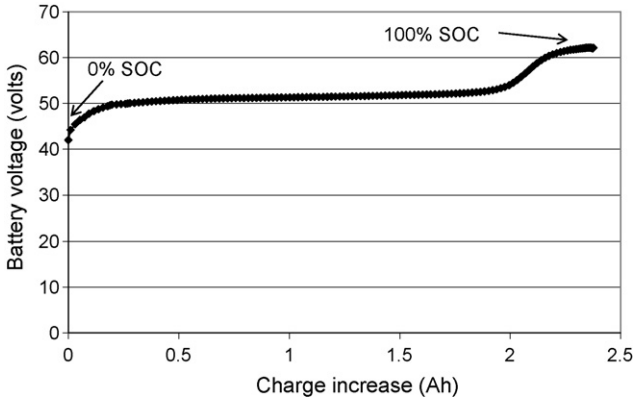

Fig. 1. Measuring charge capacity during solar charging of a 15-cell A123 Li-ion battery module.

Four battery modules could be charged simultaneously on one day in experiments under sunny, clear solar conditions using four identical solar PV modules. The first study included tests of modules with 10-, 12-, 14-, and 16-cells in series, while the second study on included tests of modules with 13-, 14-, 15-, and 16-cells in series. The current, voltage, and battery charge of a 15-cell battery module during the second study are shown in Fig. 2.

The efficiency of solar energy to battery charge conversion for the second study (13-, 14-, 15-, and 16-Li-ion cells in series) is shown in Fig. 3. The efficiency was determined at 20 s intervals by the DAQ system based on Eq. (6). The efficiency results for each battery module in both studies were averaged and are shown in Fig. 4 . For example, the charge efficiency (%) is calculated from the average voltage during each data time interval multiplied by the increase in charge (ampere hours, Ah) and divided by the time interval (converted to hours), the area of a PV module (m^2), and the average solar irradiance ($W\,m^{-2}$). A sample calculation is shown below for a 20-s data collection period and one Sanyo solar module with an

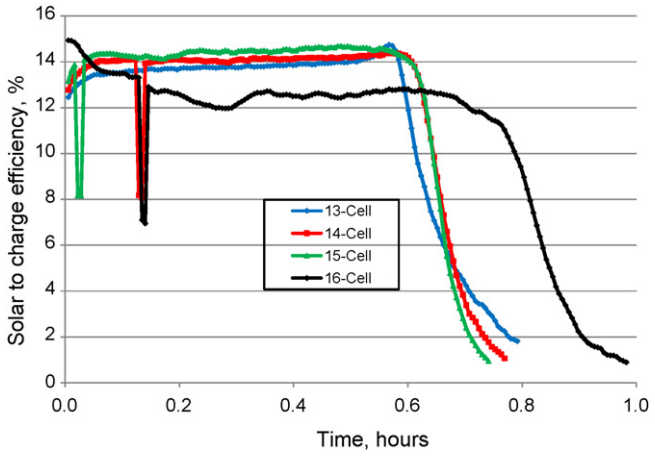

Fig. 3. Solar energy to battery charge efficiency comparison for 13-, 14-, 15-, and 16-cells in series (battery modules) as a function of time.

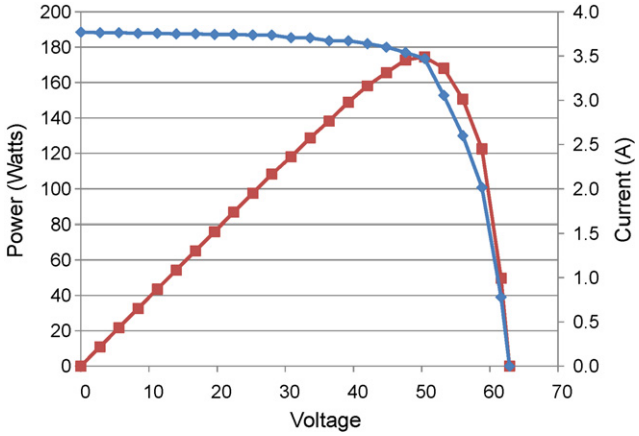

Fig. 5. Current (diamonds) and power (squares) as a function of voltage for a Sanyo HIP-190BA3 module at 52 °C. Notice the marked decrease in the current and power output for battery charge voltages above the MPP voltage at approximately 50 V.

area of 1.179 m^2:

$$\text{charge efficiency}\,(\%) = \frac{100\% \times 0.5 \times (V_2 + V_1) \times (\text{charge}_2 - \text{charge}_1)}{(20\,\text{s}/3600\,\text{s}\,\text{h}^{-1}) \times 1.179\,\text{m}^2 \times 0.5 \times (\text{irradiance}_1 + \text{irradiance}_2)}$$

A typical charge efficiency (%) of 15-cell battery module for one 20-s time step:

$$= \frac{100\% \times 0.5 \times (51.92\,\text{V} + 51.95\,\text{V}) \times (1.8464\,\text{Ah} - 1.8270\,\text{Ah})}{(20\,\text{s}/3600\,\text{s}\,\text{h}^{-1}) \times 1.179\,\text{m}^2 \times 0.5 \times (997\,\text{W}\,\text{m}^{-2} + 993\,\text{W}\,\text{m}^{-2})} = 15.5\%$$

3.2. Solar to battery charging efficiency optimization

3.2.1. Solar to charge efficiency

The highest solar energy to charge efficiency (14.5%) was achieved when the 50.2 V solar PV module was connected to the 15-cell battery module (Fig. 4). Notice the marked decrease in the solar to charge efficiency for the 13-, 14-, 15-, and 16-cell modules in Fig. 3 for times of 0.6–0.8 h into the test. This decrease occurred when the battery charging voltage surpassed the PV maximum power point (MPP) voltage (about 50 V for the test conditions). As shown in Fig. 5, the PV power decreases dramatically at voltages higher than the PV MPP. A unique phenomenon of PV cells and sets of cells (modules) is that they reach a maximum power point at a voltage slightly below the open circuit voltage. For example, under our test conditions V_{mpp} was 50.2 V and V_{oc} was 62 V (Table 2 and Fig. 5). The MPP is a result of the physical processes occurring at the p–n junction in the PV cells, involving light absorption, charge generation, charge carrier lifetime and recombination, the semiconductor band gap, and the electrical characteristics of the overall PV cell [19].

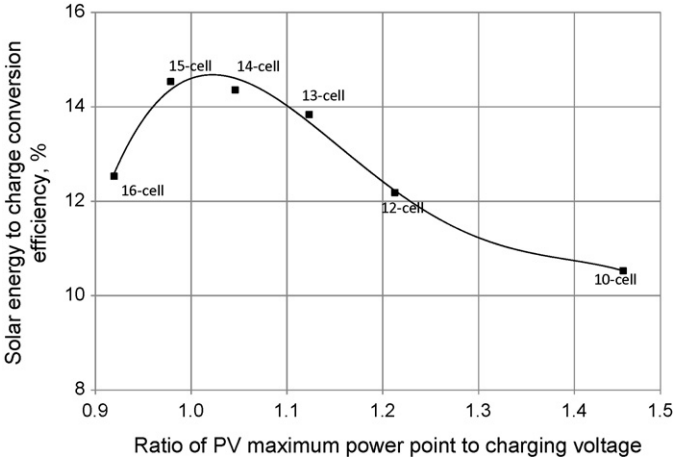

Fig. 4. Solar energy to battery charge conversion efficiency comparison for 10-, 12-, 13-, 14-, 15-, and 16-cell modules. The optimum efficiency was approximately 14.5% when the battery charge voltage was equal to the PV MPP ($V_{mpp}/V_{\text{battery charging}}$ near unity).

The effect of matching the maximum power point (MPP) voltage of the PV system with the charge voltage of the lithium-ion battery module is shown by plotting the solar energy to battery charge efficiency versus the ratio of PV MPP voltage to charging voltage (voltage ratio = $V_{mpp}/V_{\text{battery charging}}$) measured at the highest plateau of efficiency from plots such as Fig. 3. The result is shown in Fig. 4. The voltage ratio for the 15-cell battery module with the highest efficiency (14.5%) was 0.97, meaning that the PV MPP voltage was slightly less than the charging voltage at which the system charged the cells. When a 14-cell battery module was charged, the PV voltage to charging voltage ratio was slightly higher than the MPP voltage (1.05), and the efficiency was very slightly less (14.4%). When 10-, 12-, 13-, and 16-cell strings were tested, the PV voltage to charging voltage ratio moved farther away from unity indicating that the PV voltage no longer matched the charging voltage demanded by the cells. The efficiency dropped to 10.5% for the 10-cell module as the difference between the solar module MPP and the battery charging voltage increased (Fig. 4). The charge conversion efficiency curve fit to the data shows a broad maximum approaching 15% for between 14 and 15 battery cells in series at a voltage ratio of one (charging the battery at the PV MPP).

The overall conversion of solar energy to battery charge for EREV (approaching 15%) is even higher than the solar to hydrogen to fuel-cell electricity route for FCEV, because the FCEV pathway includes a solar to hydrogen process (electrolysis) with about a 10% efficiency [13], and a hydrogen to fuel-cell electricity efficiency of about 50%, for an overall efficiency of about 5% (Eq. (3)). Thus, the solar battery charging route for Li-ion batteries is approximately three times

as efficient as the route involving hydrogen for a solar energy to wheels (propulsion energy) comparison.

3.2.2. Solar charging optimization

The solar charging efficiency can be optimized by building a PV system with MPP that matches the load, which is the voltage of the battery module during charging (the battery charging voltage). Since the number of battery cells in series is determined for a particular use and operating voltage, the design and charging voltage of the solar charger are also fixed. Thus, it is necessary to design a solar PV charging system with a MPP voltage very near, but slightly below, the maximum desired battery charging voltage [17,18]. This can be accomplished by designing the PV array with a specific number of solar cells and voltage. Each solar cell in a Sanyo HIP-190BA3 module has a MPP voltage of 0.523 V at a typical operating temperature of 52 C. The standard solar module, with 96 cells in series, has a voltage of 50.2 V. PV modules could also be constructed with N number of cells in series to provide $N \times 0.523$ V to match the voltages of other battery modules designed with different charging voltages.

3.2.3. Solar charging temperatures and system self-regulation

A major concern during battery charging comes from the risk of overcharging and the resultant heat generation. In our solar charging experiments, the temperature of the Li-ion cells never rose more than slightly above ambient, sometimes reaching 30 C. The mild charging conditions occur because the PV power drops sharply when the system voltage is taken above the MPP as the battery charge approaches its capacity (100% SOC). This phenomenon is illustrated by Fig. 5, which shows the sudden decrease in power and current after the battery charge voltage rises above the PV MPP. Because of this sudden decrease, the solar charging process we developed in this work has a self-regulating capability. Using a direct connection of a battery to solar PV power in which the PV MPP is slightly below the battery charging voltage for an SOC approaching 100% will significantly reduce the risk of thermal damage to battery systems during charging. Charging current from our solar PV system was limited to 3.47 A by its inherent maximum power output (Table 2). A greater thermal risk would occur from battery discharge during a short circuit when current flow can exceed the maximum cell discharge current of 60 A [17]. This could then lead to melting the connectors between cells or heat damaging the cell casings and contents [17,18]. Another reason why we did not experience significant battery heating was the open construction of the battery modules which left open space between adjacent cells so that heat could escape easily. Battery modules built for use in vehicle battery packs would not have as open a construction and might be more subject to overheating although battery packs may be designed to dissipate heat in other ways. The rapid drop in charging rate (self-regulation) which we observed when the battery charging voltage exceeded the PV MPP is also shown in Fig. 2.

4. Summary and conclusions

Solar energy can provide a clean, renewable source of electrical energy to charge the Li-ion batteries in future EREV such as the Chevrolet Volt. This report contains a proof of concept for an optimized and safe PV-battery charging system for homes and commercial systems by utilizing a direct connection (no intervening electronics) between the PV and Li-ion battery system. The iron phosphate type Li-ion cells, tested in our study, were wired in series to create battery modules that were charged at a rate of up to 1.5 C (full charge in about 40 min). The coupling of the PV and battery systems was optimized by matching the maximum power point voltage output of the PV system at the PV operating conditions to the maximum charge voltage of the battery. This maximized the solar energy to battery charge efficiency. The optimized solar charging system efficiency reached 14.5%, by combining a 15% PV system solar to electrical efficiency and a nearly 100% electrical to battery charge efficiency. The solar Li-ion battery charging is approximately three times as efficient at providing electricity to propel an EREV as solar hydrogen is for FCEV propulsion on a solar energy to wheels (propulsion energy) basis. The rapid drop in power from the PV system as the battery voltage passed the PV maximum power point provided a self-regulating feature to the system, preventing overcharging the batteries and the potential risks of excessive heat and battery damage. A direct connection, optimized, and self-regulating PV solar battery charging system can provide an attractive pathway for providing the energy for future vehicles powered by batteries.

References

[1] G.W. Crabtree, N.S. Lewis, Physics Today 60 (2007) 37–42.
[2] J.A. Turner, Science 305 (2004) 972–974.
[3] J.A. Turner, G. Sverdrup, M.K. Mann, P.C. Maness, B. Kropski, M. Ghirardi, R.J. Evans, D. Blake, International Journal of Energy Research 32 (2008) 379–407.
[4] S.Z. Baykara, International Journal of Hydrogen Energy 30 (2004) 545–553.
[5] M. Verbrugge, P. Liu, Journal of Power Sources 174 (2007) 2–8.
[6] D.O.E., Energy Storage Research and Development, January, 2009, www1.eere.energy.gov/vehiclesandfuels/pdfs/program/2008_energy_storage.pdf.
[7] M. Broussely, G. Archdale, Journal of Power Sources 136 (2004) 386–394.
[8] D.P. Birnie III, Journal of Power Sources 186 (2009) 539–542.
[9] National Research Council/National Academy of Engineering, Hydrogen Economy: Opportunity, Costs, Barriers, and R&D Needs, National Academy Press, Washington, DC, 2004.
[10] D.R. Simbeck, E. Chang, Hydrogen Supply: Cost Estimate for Hydrogen Pathways—Scoping Analysis. Report NREL/SR-540-32525, National Renewable Energy Laboratory, Golden, CO, 2002.
[11] D. Ipsakis, S. Voutetakis, P. Serferlis, F. Stergiopoulos, C. Elmasides, International Journal of Hydrogen Energy 34 (2009) 7081–7095.
[12] L.D. Burns, J.B. McCormick, C.E. Borroni-Bird, Scientific American 287 (2002) 64–73.
[13] N.A. Kelly, T.L. Gibson, D.B. Ouwerkerk, International Journal of Hydrogen Energy 33 (2008) 2747–2764.
[14] T.L. Gibson, N.A. Kelly, International Journal of Hydrogen Energy 33 (2008) 5931–5940.
[15] A123 Systems, Proper Operation of A123 Systems High Power Lithium-ion Battery Strings, 2008.
[16] Sanyo Energy (USA) corp., HIT Series Data Sheet, HIP-190BA3, <us.sanyo.com/solar/>.
[17] C. Simpson, National Semiconductor (2007).
[18] I. Buchmann, Cadex (2001).
[19] J.L. Gray, The physics of the solar cell, in: A. Luque, S. Hegedus (Eds.), Handbook of Photovoltaic Science and Engineering, Wiley, New York, 2003, pp. 61–111 (Chapter 3).